PERIODICO di MINERALOGIA Volume 92, No. 6, 2023
ISSN: 0369-8963

Interaction Energy, Counterpoise-Corrected Energy, And Charge Transfer Thiophene Characteristics As Basis For Its Potential Use As A Gas Sensor: A Density Functional Theory Approach

HARIPRIYA P [*1], AMRUTHA R [*2] and CHANDRAN P [*3]

[*1] *Research Scholar, Bharathiar University, Coimbatore, PIN-641046, Tamil Nadu, India.*

[*2]*Department of Physics, KCG College of Technology, Rajiv Gandhi Salai, Karapakkam, Chennai, PIN-600097, Tamil Nadu, India.*

[*3] *Madras Christian College, Tambaram East, Tambaram, Chennai, PIN-600059, Tamil Nadu, India.*

[*]*Corresponding author e-mail:amrutha@kcgcollege.com*

Abstract

The gas sensing ability of thiophene has been discussed earlier, but various properties such as the interaction energy, counterpoise-corrected energy, and charge transfer based on Mulliken and natural bond orbital analysis between the analyte carbonyl sulfide (COS) and the monomer have been largely unexplored. The interaction of thiophene with COS was investigated using the density functional theory at the routes of B3LYP and ωB97XD with the basis set 6-31+G(d) level. COS gas sensors are highly desirable as these types of gaseous emissions cause acute toxicological hazards to humans and animals. When toxic COS is exposed to thiophene, it alters the electronic charge concentration, thereby changing the resistance of the host layer. Theoretical recovery times were calculated to estimate the reusable efficiency of the thiophene/COS gas sensor. Our computational studies indicate the physisorption of COS on thiophene which is confirmed by the adsorption energies and changes in the geometric, energetic, and electronic properties, thereby revealing the compound's sensing ability. The results are supported by UV-vis spectroscopic analysis. The characteristic peaks of the IR vibrational spectra are obtained.

Keywords: *Density functional theory, Thiophene, Carbonyl sulfide, Frontier molecular orbital, Global reactive indices, Ultraviolet-visible-Time dependent density functional theory.*

 https://doi.org/10.37896/pd92.6/92618

ISSN: 0369-8963

Introduction

A preprint has previously been published. [Haripriya et al. 2022] [1].

Conjugated organic polymers (COPs) are conducting polymers owing to the presence of delocalized π-orbital electrons. Many COPs, including polyaniline, polythiophene, polypyrrole, polyparaphenylene, polyphenylenevinylene, and polyphenylene sulfide, are used in the fields of energy storage [2] and in electronic chemical sensors [3]. The applications of conducting polymers in various sensors are considerably fascinating. Conducting polymers exhibit excellent electrical conductivity characteristics and have been applied extensively in field-effect transistors [4]. Salient features of conducting polymers and the application of conducting polymers to biosensors in the field of health care, food industries, and environmental monitoring were studied by Gerard et al. [5]. The excellent electrical conductivity of polyselenophene and their applications in electronic devices (e. g., actuators) were reported by Patra et al. [6]. Patois et al. investigated the influences of the electropolymerization parameters on the ammonia gas detection efficiency of polypyrrole-based sensors. [7]. The use of conducting polymers (as emerging commercial materials) and their applications in batteries, gas sensors, electromagnetic interference shielding, light-emitting diodes, and solar cells, were studied by Kumar et al. [8]. The gas sensing property induces polymer conductivity changes due to the alteration of the doping levels of the conducting polymer attributed to the transfer of electrons from or to the analytes [9]. The sensing properties of conjugated organic polymers with various gas molecules and their structural and electronic properties have been studied extensively computationally [10–15]. Among all the COPs, polythiophene and its derivatives are attractive owing to their excellent electrical, chemical, and physical properties. Polythiophene, which is used in electrochromics and conducting polymer films, has improved gas sensing properties compared with other

 https://doi.org/10.37896/pd92.6/92618

ISSN: 0369-8963

COPs. Polythiophene has numerous derivatives, such as poly (3, 4- ethylenedioxythiophene) (PEDOT), which has a conducting polymer with a moderate band gap, low redox potential, and optical transparency characteristics, and has been extensively applied in energy conversion and storage devices.

In our previous research work, intermolecular charge transfer between COS and thiophene enabled us to elucidate the adsorption phenomenon between the donor (COS) and the acceptor(thiophene). [16]. The above mentioned study investigated the second order perturbation theory of Fock matrix of the interacting NBOs, and the population of electrons in the core, valence, and Rydberg subshells was analyzed by density functional theory. Further, our previous work on NBO analysis confirmed the charge transfer from the lone pair of oxygen of COS to σ* of C_1-H_6 of thiophene that led to adsorption . Continuation of our previous work, in this present work, the sensing ability of thiophene with COS is proved by its structural parameters that are supported by interactions and counterpoise-corrected energies. Various structural and electronic properties, such as inter- and intrabond lengths, bond angles, interaction energy, counterpoise corrected energy, charge transferring phenomena by Mulliken and NBO analyses, dipole moment, highest occupied molecular orbital (HOMO), lowest unoccupied molecular orbital (LUMO), and energy gap, are calculated for the adsorbed analyte thiophene to show that the COS interacts well with thiophene, making it less chemically stable and more reactive. Part of the success of our approach is attributed to the fact that DFT provides a strong foundation to study chemical reactivity calculated based on simple equations that describe various global indices of reactivity, such as the ionization potential, electron affinity, softness, electrophilicity, hardness, electronegativity, and chemical potential. Analyses of excited state properties, such as UV-vis spectroscopic analysis were performed by , and the results correlate strongly with our theoretical work that reflects the electronic properties of the monomer. The IR vibrational

 https://doi.org/10.37896/pd92.6/92618

ISSN: 0369-8963

properties are simulated at DFT B3LYP/6-31+G (d) level and the IR assignments of monomer and monomer with analyte are strongly correlated with experimental frequencies. Our results indicate that COS interacts with thiophene based on a physisorption process owing to the existence of van der Waals forces between the monomer and the analyte. We believe that our study makes a significant contribution to the literature because gas sensors used to detect COS gas are highly desirable as they eliminate acute toxicological hazards to humans and animals [17, 18]. It was also reported that under repeated exposure of COS gas will reversibly harm male fertility and at prolonged exposure it could be neurotoxic. [19]. Thus, the action of COS with the nervous system is quite remarkable. The gas COS can be used an intermediate of sulfur containing herbicides and can be used as a fumigant in the agricultural industry. [20]. Since the gas poses a significant public health risk , it should be eliminated from the environment. Thus our studies are towards COS sensing and our work mitigate the significant public health risk by detecting the toxic gas which causes numerous health problems.. Further, the electronic property of the polythiophene monomer that facilitates the withdrawal of an electron from the analyte reduces the HOMO-LUMO gap that enhances high-charge carrier mobility; these changes are very helpful in the design of organic light-emitting diodes.

Our study will provide a better platform to advance additional research efforts pertaining to the analysis of the gas-sensing behavior of polythiophene with COS in various fields of optoelectronics. Overall, our research findings suggest that thiophene is a very effective COS sensor.

One of the main objectives of our work is the hitherto unexplored determination of the decrease in the energy gap of thiophene after interactions with COS, as it increases the electrical conductivity of thiophene and makes it suitable for use in organic cells and organic light-emitting diodes. Thus, we report that the interaction between the monomer and analyte

 https://doi.org/10.37896/pd92.6/92618

ISSN: 0369-8963

changes the electronic structure of thiophene that induces changes in the electrical conductance; this alteration can be transformed into a signal to allow it to develop as a new sensor. To the best of our knowledge, this area has been largely unexplored, and exploration of these studies indicates the potential of thiophene for use as an inexpensive sensor for the aforementioned analyte.

Material and Methods

The molecular orbital theory is very useful for the description of the electronic structures of molecules. The basic framework of the MO method was proposed by Hund [21], Mulliken [22], and Lennard–Jones [23] and enables us to interpret the nature of the ground and excited states of molecules. All calculations were performed in the gas phase using "Gaussian 09 [24]," and the results were analyzed using the GaussView (version 5. 0), [25], and the Gabedit computer programs (version 2. 5. 0, A. R. Allouche) [26]. The geometries of thiophene, COS, and the complex were optimized with the DFT method using the B3LYP/6-31+G(d) basis set. Various configurations of the complex (thiophene with analyte) were considered and were allowed to relax, and the most stable configuration(minimum energy)was used for calculation after relaxation. Frequency analysis was performed for the optimized structure to ensure that these stable structures corresponded to true minima, and the stationary points were confirmed to have no imaginary frequencies. Moreover, for comparison purposes, we used the best hybrid ωB97XD/6-31+G(d) level of theory [27] in conjunction with Grimme's D2 dispersion model [28] for the optimization of structures. As the DFT of functional B3LYP/6-31+G(d) does not consider the dispersion arising from the fluctuation of the charge distribution around a molecular system due to the movement of the electrons, the ωB97XD/6-31+G(d) functional was used. The ωB97XD functional should be appropriate because of its long-range, corrected exchange-correlation behavior with the inclusion of Grimme dispersion correction [29]. It is well known that the DFT Becke's three-

 https://doi.org/10.37896/pd92.6/92618

ISSN: 0369-8963

parameter exchange functional in conjunction with the Lee-Yang-Parr correlation functional B3LYP level [30–33] with the well-accepted basis set, 6-31+G(d), will yield accurate results because of its exchange correlation property. Our previous work on the molecular orbital calculation on the structures of mono- and dihydroxy benzenes and their halogen substituted species showed that the DFT B3LYP method provides more accurate molecular structure predictions [34].

The interaction energy between thiophene and analyte is calculated by Eq. (1)

$$E_{int} = E_{complex} - \left(E_{monomer} + E_{analyte}\right) \quad (1)$$

The interaction energy is corrected by the counterpoise method expressed by Eq. (2)

$$E_{int,CP} = E_{int} - E_{BSSE} \quad (2)$$

where $E_{complex}$ is the total energy of the optimized thiophene with COS physiosorbed on it, $E_{monomer}$ is the total energy of the isolated thiophene molecule, $E_{analyte}$ is the total energy of the gaseous COS, and E_{BSSE} and $E_{int,\ CP}$ represent the basis set superposition error and counterpoise-corrected interaction energies of the complex, respectively. E_{int} is calculated after the energies of the systems attain their relaxed minimum structures.

The recovery time can be calculated by the following equation [35,36],

$$\tau = \nu^{-1}\exp\left[\frac{|E_b|}{k_b T}\right] \quad (3)$$

where ν can be interpreted as the attempt frequency to break the bond. The frequency ν is typically around 1THz, E_b is the binding energy of the gas on the thiophene, T=300K, and k_b is Boltzmann's constant.

 https://doi.org/10.37896/pd92.6/92618

ISSN: 0369-8963

Results and Discussion

In recent years, computational studies have been performed to assess the sensing ability of thiophene with different gases [13] and determine the interaction with several toxic gases, such as carbonyl sulfide with polypyrrole. [37]. However, in the case of the polythiophene monomer and its interactions with COS, various structural and electronic properties before and after the interaction, and especially the global reactive indices, have not been studied previously. In our present work, quantum chemical calculations were carried out to investigate the adsorption characteristics of monomer of polythiophene with COS, and a comparison and study of the geometric and electronic properties to establish thiophene as a more useful sensor were also carried out.

Inter- and intrabond lengths and bond angles

Geometries of the isolated thiophene, COS, and the complex, were optimized at the DFT B3LYP/6-31+G(d) level, and the results of the monomer were compared with the available experimental values [38, 39] to describe the correlation between the geometric structures and its properties. The optimized structures of thiophene, COS, and thiophene with COS are shown in Figures1(a), 1(b), and 1(c), respectively. We found that the intrabond lengths and bond angles calculated for the monomer at the B3LYP/6-31+G(d) level correlate well with the experimental values with the appropriate choice of basis set listed in Table 1. The difference between the experimental and the calculated bond length for C=C is 0. 0004 Å.

The C-S and C-C bond lengths from our findings slightly differ compared with the experimental values by 0. 0216 Å and 0. 0078Å, respectively. There is an increase in the value of C-H bonds nearest to the sulfur by 0. 0042Å. The C_2-H_7 and C_3-H_8 bonds vary by 0. 0041Å. The calculated bond angles ∠C-C-S and ∠C-C-C are slightly higher than the experimental values by 0. 0902° and 0. 1704°, respectively, whereas the ∠C-S-C bond angle

 https://doi.org/10.37896/pd92.6/92618

ISSN: 0369-8963

is slightly less than the experimental value by 0. 66°. The bond angles ∠C-C-H and ∠S-C-H differ from the experimental values by 0. 35° and 0. 19°, respectively. The results obtained from the DFT at the level of B3LYP/6-31+G(d) calculations are in good agreement with the experimental values [38, 39] which substantiate the accuracy of the basis set.

The optimized geometrical parameters of the complex undergo changes in the bond lengths and the bond angles with respect to those of the monomer, thereby establishing the sensitivity and selectivity of the monomer with the analyte. The C_1-C_2 bond length of the complex decreases by 0. 0001Å compared with that of the monomer and the same trend is observed for the C_1-S_5 bond. The C_1-H_6 bond length for the complex is smaller than that of the monomer by 0. 0003 Å. The C_2-C_3 bond length of the complex gradually increased, and the maximum difference was 0. 0001Å that of the monomer. There were no remarkable changes in the bond lengths for C_2-H_7, C_3-C_4, and C_3-H_8, and there was slight elongation of the bond lengths for C_4—S_5 and C_4—H_9 by 0. 0002 Å and 0. 0001Å, respectively.

The bond angles of the complex ∠$C_2C_1S_5$, ∠$S_5C_1H_6$, ∠$C_1C_2H_7$, ∠$C_2C_3C_4$, ∠$C_4C_3H_8$, ∠$C_3C_4S_5$, and ∠$C_3C_4H_9$ were smaller with respect to those of the monomer by 0. 0328°, 0. 297°, 0. 0561°, 0. 0252°, 0. 0053°, 0. 0091°, and 0. 0789°, respectively, whereas a different trend was observed for the bond angles ∠$C_2C_1H_6$, ∠$C_1C_2C_3$, ∠$C_3C_2H_7$, ∠$C_2C_3H_8$, ∠$S_5C_4H_9$, and ∠$C_1S_5C_4$ which were larger than that of the monomer by 0. 3299°, 0. 0482°, 0. 0078°, 0. 0304°, 0. 0881°, and 0. 0189°, respectively. It is observed that both the interior and exterior intramolecular bond angles alternatively decrease and increase with respect to those of the monomer owing to the influences of the interaction sites, namely, C_{11} of COS and S_5 of thiophene. The exterior bond angles ∠$C_3C_2H_7$ and ∠$C_2C_3H_8$, which are far away from the interaction site are overestimated than that of the monomer. The geometric changes in the bond angles are produced due to the appreciable internal strain that arises owing to the inclusion of d-atomic orbitals in the basis set for both the monomer and analyte. The bond

 https://doi.org/10.37896/pd92.6/92618

ISSN: 0369-8963

angle $\angle S_5C_4H_9$ that is closer to the S-side of COS widens, whereas the bond angle $\angle S_5C_1H_6$ that is closer to the O-side of COS was underestimated. After the optimization of the complex, the bond angle $\angle S_5C_1H_6$ narrowed because it was closer to the interaction site of COS. The changes in the bond angle of the complex involving S_5 of thiophene are attributed to its electronegative property that influences the analyte, and results in the alteration of its structural parameters. Furthermore, the bond angle in the electronic structure of the complex changes owing to the existence of a van der Waals force between the monomer and analyte. Moreover, the polarity of COS also changed the bond angle of the monomer based on dipole-induced–dipole interactions. The polarity of the analyte changed the orientation of the monomer. Our studies revealed that only slight changes in the bond lengths and bond angles of the complex occurred compared with that of the isolated thiophene after interaction, which is normally associated with the lowest negative interaction energy value.

The optimized interbond length and the various interaction bond angles of the complex are listed in Table 2. The interaction distance is very important in connection with the interaction site between S_5 of thiophene and C_{11} of COS; its value is 4. 5932Å. The optimized inter- and intramolecular interactions produce considerable changes in their values, thus revealing the interaction between the monomer and the analyte.

 https://doi.org/10.37896/pd92.6/92618

ISSN: 0369-8963

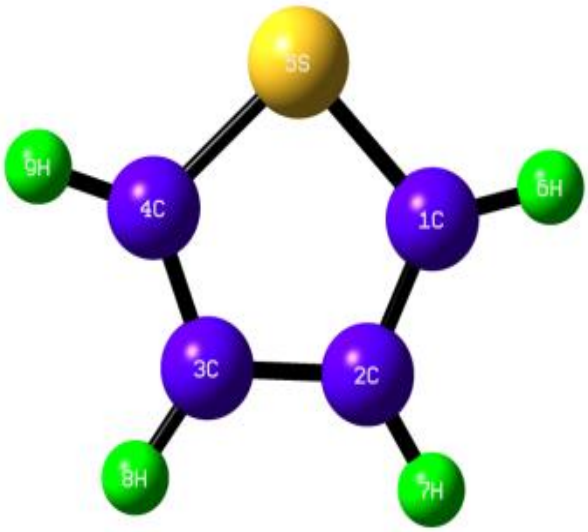

1 (a)

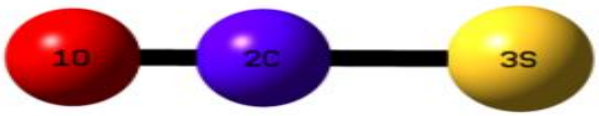

1(b)

https://doi.org/10.37896/pd92.6/92618

ISSN: 0369-8963

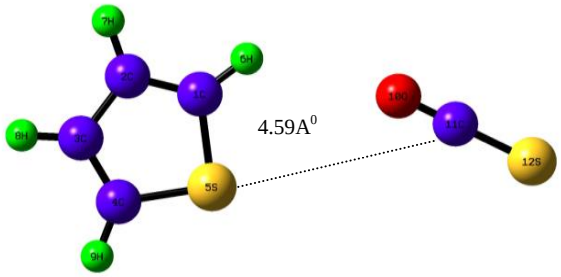

1(c)

Figure 1. (a) Optimized structure of thiophene at the density functional theory (DFT) B3LYP/6-31+G (d) level. **1.(b)** Optimized structure of carbonyl sulfide (COS) at the DFT B3LYP/6-31+G (d) level. **1.(c)** Optimized structure of thiophene with COS at the DFT B3LYP/6-31+G (d) level. The violet, green, yellow, and red balls represent C, H, S, and O, respectively

https://doi.org/10.37896/pd92.6/92618

ISSN: 0369-8963

Table 1. Optimized intrabond lengths [in Å] and bond angles in [°] calculated at the density functional theory (DFT) B3LYP/6-31+G(d) level

Serial. Number (S. no)	Thiophene		Thiophene with carbonylsulfide (COS)		Experimental value of thiophene
	Parameter	Value	Parameter	Value	
1	C_1-C_2	1. 3704	C_1-C_2	1. 3703	1. 370
2	C_1-S_5	1. 7356	C_1-S_5	1. 7355	1. 714
3	C_1-H_6	1. 0822	C_1-H_6	1. 0819	1. 078
4	C_2-C_3	1. 4308	C_2-C_3	1. 4309	1. 423
5	C_2-H_7	1. 0851	C_2-H_7	1. 0851	1. 081
6	C_3-C_4	1. 3704	C_3-C_4	1. 3704	1. 370
7	C_3-H_8	1. 0851	C_3-H_8	1. 0851	1. 081
8	C_4 -S_5	1. 7356	C_4 -S_5	1. 7358	1. 714
9	C_4-H_9	1. 0822	C_4-H_9	1. 0823	1. 078
10	$\angle C_2C_1S_5$	111. 5602	$\angle C_2C_1S_5$	111. 5274	111. 47
11	$\angle C_2C_1H_6$	128. 3506	$\angle C_2C_1H_6$	128. 6805	-
12	$\angle S_5C_1H_6$	120. 0891	$\angle S_5C_1H_6$	119. 7921	-
13	$\angle C_1C_2C_3$	112. 6704	$\angle C_1C_2C_3$	112. 7186	112. 5
14	$\angle C_1C_2H_7$	123. 3806	$\angle C_1C_2H_7$	123. 3245	-
15	$\angle C_3C_2H_7$	123. 9491	$\angle C_3C_2H_7$	123. 9569	124. 3
16	$\angle C_2$ C_3C_4	112. 6704	$\angle C_2$ C_3C_4	112. 6452	-
17	$\angle C_2C_3H_8$	123. 9491	$\angle C_2C_3H_8$	123. 9795	-
18	$\angle C_4C_3$ H_8	123. 3806	$\angle C_4C_3$ H_8	123. 3753	-
19	$\angle C_3C_4$ S_5	111. 5602	$\angle C_3C_4$ S_5	111. 5511	-

https://doi.org/10.37896/pd92.6/92618

ISSN: 0369-8963

20	$\angle C_3C_4H_9$	128. 3506	$\angle C_3C_4H_9$	128. 2717	-
21	$\angle S_5C_4H_9$	120. 0891	$\angle S_5C_4H_9$	120. 1772	119. 9
22	$\angle C_1\ S_5\ C_4$	91. 5388	$\angle C_1\ S_5\ C_4$	91. 5577	92. 2

Table 2. Optimized inter bond lengths [in Å]and bond angles [in °] of thiophene with carbonyl sulfide (COS)calculated at the DFT B3LYP/6-31+G(d) level

Parameter	Value
S_5-C_{11}	4. 5932
O_{10}-C_{11}	1. 1672
C_{11}-S_{12}	1. 5707
$\angle C_1\ S_5\ C_{11}$	82. 5288
$\angle\ C_4S_5C_{11}$	170. 6447
$\angle\ S_5\ C_{11}\ O_{10}$	41. 4068
$\angle\ S_5\ C_{11}\ S_{12}$	138. 6448

Interaction energy and the counterpoise-corrected energy

Gas adsorption is helpful in determining the adsorption energy and the amount of charge transferred between the monomer and the analyte. The value of the interaction energy calculated for thiophene with COS is listed in Table 3. The interaction energy value between thiophene and COS is exothermic and is equal to -2. 0083 kJ/mol; it is clear from the value that the COS molecule can be adsorbed physically on the monomer. The intermolecular nonbonding distance between the sulfur of thiophene and carbon of COS is 4. 5932Å (see Table 2), which supports the van der Waals type of interaction. The value of the interaction

 https://doi.org/10.37896/pd92.6/92618

ISSN: 0369-8963

energy is in the range of the physisorption process. A lower value of adsorption energy results in a shorter adsorption distance [40]. However, in our results, we obtained a higher value of adsorption energy, or alternatively, the lowest negative value of interaction energy in a longer adsorption distance. The minimum negative value of the interaction energy proves the existence of the van der Waals force [15] that is generated between the sulfur of thiophene and the carbon of COS, and reveals the physical adsorption process that occurs during the intermolecular interaction. The interaction energy value calculated for thiophene with COS at DFT ωB97XD/6-31+G(d) level is listed in Table 4 and was equal to -11. 0198kJ/mol. Our result shows that the interaction energy at the DFT ωB97XD/6-31+G(d) level is somewhat higher than that at the DFT B3LYP/6-31+G(d) level. This is attributed to the fact that for functionals for smaller systems consisting of 4–8 atoms, the inclusion of dispersion corrections always increases the root-mean-square (RMS)interaction energy error [29].

The interaction energy was corrected by the counterpoise-corrected energy method; this is expressed by Eq. (2). The counterpoise-corrected energy value for the adsorption of thiophene with COS= -1. 1297 kJ/mol, indicating that a relatively weak interaction has occurred. At the DFT ωB97XD/6-31+G(d) level, the counterpoise-corrected interaction energy was equal to -9. 4977 kJ/mol. For weakly bound complexes, we can see that the basis set superposition error energy value of 0. 8816kJ/mol is observed at an interaction energy of the order of 0.78% based on the DFT B3LYP/6-31+G(d) level; in addition, a BSSE value equal to1. 397 kJ/mol of energy of the order of 0. 147% of E_{int} was observed at the ωB97XD/6-31+G(d) theory level. The calculated nuclear repulsion energy (E_{NN}) for thiophene at the ωB97XD/6-31+G(d) level was equal to 531426. 4048 kJ/mol and for the complex E_{NN} was equal to 1192060. 7953 kJ/mol.(Refer Table 4).The reported E_{NN} from the literature for thiophene at ωB97XD/3-21G* was equal to 531435. 331 kJ/mol, at ωB97XD/6-

 https://doi.org/10.37896/pd92.6/92618

ISSN: 0369-8963

31+G**, the value was 531569. 232 kJ/mol, and at ωB97XD/6-311G**, the value was 532645. 687 kJ/mol [41]. These outcomes provide strong support toward the reliability of our computed values. The nuclear repulsion energy increased by a value of 660634. 391kJ/mol for the complex than isolated thiophene with empirical dispersion; this implies a greater repulsive force for the complex after interaction, thereby emulating the dispersion. The quantity minimized during the geometry optimization is the total energy of the molecular system that could compensate an increase in the value of nuclear repulsion energy.

The recovery time of thiophene after interaction with the gas at the DFT B3LYP/6-31+G(d) level as listed in Table 3 is equal to 2. 2375 × 10^{-12}s; at the DFT ωB97XD/6-31+G(d) level, the recovery time is equal to 8. 30132 × 10^{-11} s. (see Table 4). Our measurements showed that COS adsorbed on thiophene had fast recovery times, thus proving its reusability. The recovery time for the route DFT at the level of ωB97XD/6-31+G(d) suggests a very fast recovery than that at the DFT B3LYP/6-31+G(d) level, thereby ensuring that thiophene serves as a reusable gas sensor with rapid recovery time for COS gas detection.

Charge analysis

The amount of charge transfers based on Mulliken and NBO analyses is listed in Table 3. The interaction between thiophene and COS is best explained based on the charge transfer. Charge transfer alters the electronic and structural properties of thiophene. The amount of charge transfer provides the sensing capability and selectivity of the monomer toward the analyte. Charge transfer analysis was conducted at the B3LYP/6-31+G (d) theory level. The charge transferred between thiophene and COS was calculated from the difference between the charge on thiophene after its interaction with COS and the charge on the isolated

 https://doi.org/10.37896/pd92.6/92618

ISSN: 0369-8963

thiophene. Population analysis for the Mulliken charge transfer showed that COS transferred an approximate charge equal to 0. 0149e^- to thiophene. Based on the NBO analysis, COS donated a charge equal to 0. 00023e^- to thiophene. NBO analysis provided information about the intra- and intermolecular charge transfer between the filled orbitals of one system and the vacant orbitals of another system. These charge transfer results are consistent with the results of our previous recent studies on the second-order perturbation theory of the Fock matrix of thiophene with COS obtained based on NBO analysis, whereby COS was considered as a donor NBO and thiophene as an acceptor NBO [16]. The charge transfer also altered the energy gap, resistance, HOMO, LUMO, and λ_{max} of thiophene, and thus, affected its sensitivity after interaction. Owing to the electron donating and electron accepting characteristics of the orbitals, electronic charges were delocalized over the entire system.

Table 3. Interaction energy, counterpoise-corrected energy, basis set superposition error (BSSE) energy, recovery time, and charge transfer from Mulliken and natural bond orbital (NBO) analysis calculated at the DFT B3LYP/6-31+G(d) level

S. no	Parameter	Value
1	E_{int} [kJ/mol]	-2. 0083
2	$E_{int, CP}$ [kJ/mol]	-1. 1297
3	BSSE energy [kJ/mol]	0. 8816
4	Recovery time [s]	2. 2375 × 10^{-12}
5	$Q_{Mulliken}$	-0. 0149e^-
6	Q_{NBO}	-0. 00023e^-

 https://doi.org/10.37896/pd92.6/92618

ISSN: 0369-8963

Table 4. Interaction energy, counterpoise corrected energy, BSSE energy, recovery time, and nuclear repulsion energy (E_{NN}) calculated at the DFT ωB97XD/6-31+G(d) level

S. no	Parameter	Value
1	E_{int} [kJ/mol]	-11. 0198
2	$E_{int, CP}$ [kJ/mol]	-9. 4977
3	BSSE energy [kJ/mol]	1. 3965
4	Recovery time [s]	8.30132×10^{-11}
5	E_{NN} for thiophene [kJ/mol]	531426. 4048
6	E_{NN} for thiophene with COS [kJ/mol]	1192060. 7953

Dipole moment

The values of the dipole moment of thiophene and thiophene with COS along the three coordinate axes and the net dipole moments of the monomer and monomer with analyte are listed in Table 5. It is shown that thiophene has a net dipole moment equal to 0. 5469 Debye, and thiophene with COS has a net dipole moment equal to 0. 5060 Debye. During the physisorption process, the gas molecule introduces a net dipole moment owing to the charge transfer between the gas analyte and thiophene. Both the geometric and electronic properties are related to the dipole moment. A lower value of the dipole moment for the complex is associated with a lower value of interaction energy, and a change of 0. 0409 Debye in the dipole moment value will produce a smaller shift in the allocation of electrons. As the complex possesses a lower dipole moment value than isolated thiophene, weak intermolecular interactions arise. For thiophene, the maximum value of the dipole moment is along the y-direction, but it is lower along the x-direction. For thiophene with COS, the major contribution to the dipole moment is along the x-axis, while the contribution is lower along the y-axis, and

 https://doi.org/10.37896/pd92.6/92618

ISSN: 0369-8963

the value of the dipole moment is negative along the z-direction. The orientations of the vector of the dipole moment in the molecular axis system of the monomer and the monomer with the analyte are shown in Figures 2(a) and 2(b), respectively. The monomer accepts electronic charge from the analyte, and the dipole moment vector is directed from thiophene to COS as the dipole moment vector is always directed from the negative to the positive charge, as shown in Figure 2(b). The calculated dipole moment value of thiophene closely matches the experimental value, which is equal to 0. 55 Debye [38, 39]. Thus, the calculated dipole moment values establish the measure of the electrical polarity of the system.

 https://doi.org/10.37896/pd92.6/92618

ISSN: 0369-8963

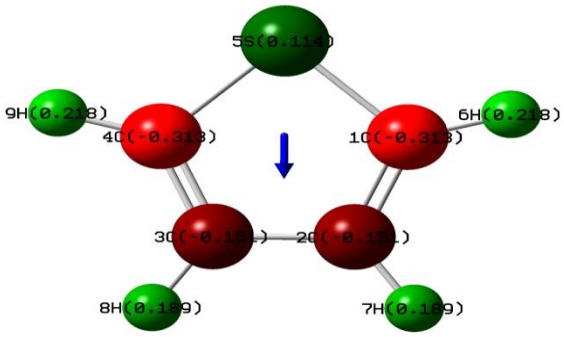

2 (a)

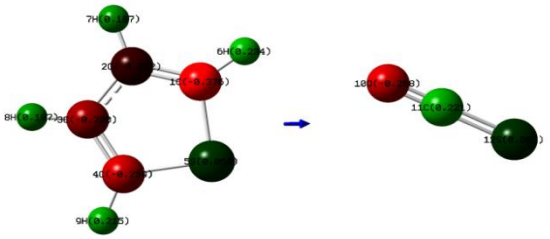

2(b)

Figure 2. (a) Dipole moment vector of thiophene at the DFT B3LYP/6-31+G(d) level. **2. (b)**Dipole moment vector of thiophene with COS at the DFT B3LYP/6-31+G(d) level

https://doi.org/10.37896/pd92.6/92618

ISSN: 0369-8963

Table 5. Dipole moment along the three coordinate axes [Debye] calculated at the DFT B3LYP/6-31+G(d) level

S. no	Direction	Dipole moment of thiophene	Dipole moment of thiophene with COS
1	X	0. 0024	0. 4828
2	Y	0. 5469	0. 0077
3	Z	0. 0000	-0. 1513
4	Total	0. 5469	0. 5060

Frontier molecular orbitals and band-gap analysis

The energies of the HOMO and LUMO and energy gap (E_g) were simulated at the B3LYP/6-31+G(d) level because of the reported accuracy of the B3LYP route. Both HOMO and LUMO are important orbitals that take part in chemical reactions. Interactions between the monomer and the analyte occur because of interactions of occupied or unoccupied molecular orbitals that lead to electrostatic/van der Waals interactions. When thiophene and COS are in close proximity, their molecular orbitals start interacting with each other owing to the overlapping of the frontier molecular orbitals (HOMO and LUMO). This leads to changes in the energies of HOMO and LUMO. The lower value of the dipole moment calculated earlier produces lower changes in the energy levels. The interaction of the molecular orbital of thiophene with the analyte will change the sensing properties of the monomer. For example, HOMO and LUMO are perturbed after the interaction process. This perturbation also affects other properties, such as the ionization potential, electron affinity, and energy gap; these are discussed in a subsequent subsection. The frontier molecular orbitals of the monomer and the monomer with analyte, and their corresponding energy gaps, are listed in Table 6. Relevant schematics showing the frontier molecular orbitals for thiophene and thiophene with COS at

 https://doi.org/10.37896/pd92.6/92618

ISSN: 0369-8963

the DFT B3LYP/6-31+G(d) level are shown in Figures 3(a) and 3(b), respectively. It is shown that HOMO is localized on the thiophene before and after complexation, thereby indicating its uniform electron density distribution in its orbitals. Conversely, COS contributes to LUMO after its interaction with the analyte. An increase of value equal to 0. 1003eV is observed in the energy of HOMO of thiophene after interacting with COS. The LUMO energy decreased by 0. 6573eV.

The energy gap is a critical parameter determining the electrical transport properties, and it is a measure of electrical conductivity. Alteration in orbital energies also alters the corresponding energy gap of the monomer. The energy gap value decreased from 5. 97 eV to 5. 21 eV after the interaction of the monomer with the analyte. The energy gap mainly decreased because of the decrease of the LUMO energy. The decrease of the band-gap value after interaction with the analyte increased the conductivity of thiophene. The lower band-gap values of the complex than that of the isolated thiophene indicate a less chemically stable and an increased reactive state.

 https://doi.org/10.37896/pd92.6/92618

ISSN: 0369-8963

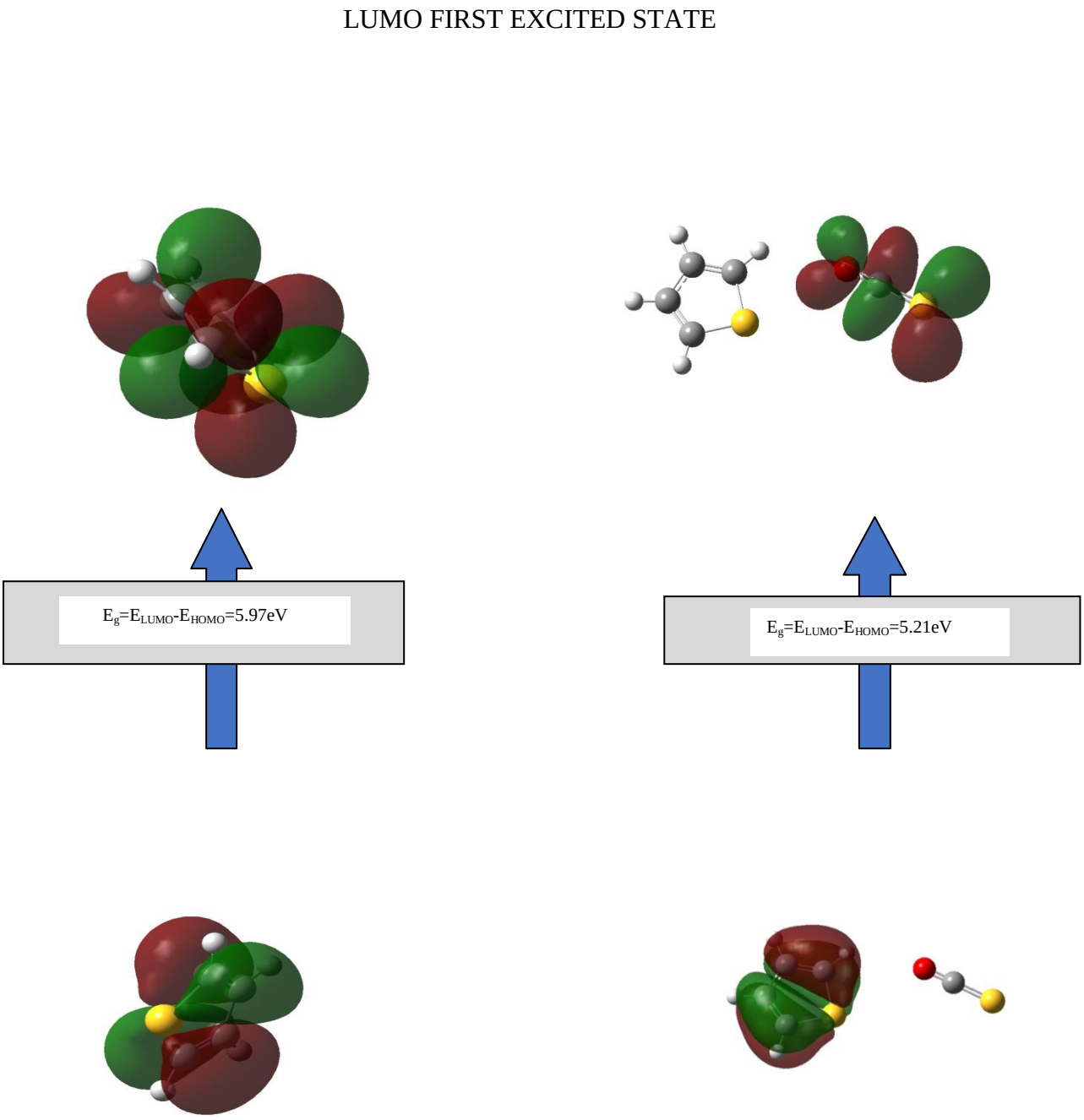

Figure 3 (a) Frontier molecular orbitals for thiophene, and (b)thiophene with COS at the DFT B3LYP/6-31+G(d) level

https://doi.org/10.37896/pd92.6/92618

ISSN: 0369-8963

Table 6. Frontier molecular orbitals [eV]and band-gap analysis [eV] calculated at the DFT B3LYP/6-31+G(d) level

S. no	Parameter	Thiophene	Thiophene with COS
1	Highest occupied molecular orbital (HOMO)	-6. 6100	-6. 5097
2	Lowest unoccupied molecular orbital (LUMO)	-0. 6397	-1. 2970
3	Energy gap E_g	5. 97	5. 21

Global reactivity indices

To calculate the global reactivity indices, such as the global hardness, softness, chemical potential, electrophilicity, and electronegativity, two important parameters, namely, the ionization potential and electron affinity, need to be calculated. It is well known that the quantum chemical parameters that are associated with the molecular electronic structure are the ionization potential (I) and electron affinity (A) of the corresponding molecules and the negative values of the DFT orbital (HOMO and LUMO) based on Koopmans' theorem [42]. The values of the ionization potential for thiophene and thiophene with COS were 6. 6100eV and 6. 5097eV, respectively. The values of electron affinity for thiophene and thiophene with COS were0. 6397eV and 1. 297 eV, respectively.

The hardness (η) can be calculated by using Koopman's theorem [42,43] as

$$\eta = \frac{E_{LUMO} - E_{HOMO}}{2} \quad (4)$$

The softness (S)is described by the following equation [43,44]

$$S = \frac{1}{2\eta} \quad (5)$$

 https://doi.org/10.37896/pd92.6/92618

ISSN: 0369-8963

The value of the chemical potential (μ) can be found by the following equation [42]

$$\mu = -\frac{(E_{HOMO}+E_{LUMO})}{2} (6)$$

Theoretically, electrophilicity (ω)is described using the following equation [44]

$$\omega = \frac{\mu^2}{2\eta} (7)$$

The global hardness (η) represents a good indicator of chemical stability. The global hardness (η) value decreased from 2. 9852eV to 2. 6064eV, which reduced the stability and increased the reactivity of thiophene after interactions with COS. The value of the chemical potential decreased by 0. 278 eV after gas sensing. The global electrophilicity (ω) also depended on the chemical potential (μ) and hardness (η). The electrophilicity index (ω) is a factor used to measure the lowering of the energy owing to the maximum number of electrons that flow between the donor and acceptor. Table 7 shows that there is an increase in the electrophilicity value (ω) from 2. 2011 eV to 2. 9227eV. It is clear that when the energy gap value is smaller than that of the isolated thiophene, the electrophilicity of the complex increases compared with that of the isolated thiophene. The global hardness (η) and softness(S) are inversely related to each other. Therefore, when the global hardness (η) value decreases, the softness value(S) increases from 0. 1675eV to 0. 1919eV. Softness(S) is a property that measures the extent of chemical reactivity. The smaller energy gap between HOMO and LUMO of thiophene with COS supports the high-chemical softness and lower value of hardness compared with that of the monomer [45]. The molecules that have a large HOMO–LUMO energy gap are called “hard molecules,” while the molecules with a small HOMO–LUMO energy gap are called “soft molecules.” The molecules with the lowest HOMO–LUMO gap become more reactive, which establishes our result. The value of electronegativity (χ) can be obtained by the equation

$$\chi = \frac{(I+A)}{2} (8)$$

 https://doi.org/10.37896/pd92.6/92618

ISSN: 0369-8963

The values of χ for thiophene and thiophene with COS were equal to 3. 6249eV and 3. 9034eV, respectively. The higher electronegativity value of the complex compared with that of the monomer reveals that there is a charge transfer from the analyte to the monomer. The Fermi level (E_{FL}) lies between the valence and conduction bands, and it is given by the equation

$$E_{FL} = \frac{(E_{HOMO}+E_{LUMO})}{2} \quad (9)$$

This means that the position of the Fermi level will be in the middle of HOMO and LUMO. Our result shows that the Fermi level value changes from -3. 625 eV to -3. 903eV upon interaction with COS.

Table 7. Global reactivity indices: ionization potential(I), electron affinity(A), global hardness(η), softness(S), chemical potential(μ), electrophilicity(ω), electronegativity(χ), and Fermi level (E_F) calculated at the DFTB3LYP/6-31+G(d) level (all parameters are in units of eV)

S. no	Parameter	Thiophene	Thiophene with COS
1	$I = -E_{HOMO}$	6. 6100	6. 5097
2	$A= -E_{LUMO}$	0. 6397	1. 2970
3	$\eta=(E_{LUMO}-E_{HOMO})/2$	2. 9852	2. 6064
4	$S=1/2\ \eta$	0. 1675	0. 1919
5	$\mu= -(E_{HOMO}+E_{LUMO})/2$	-3. 6249	-3. 9034
6	$\omega= \mu^2/2\ \eta$	2. 2011	2. 9227
7	$\chi=(I+A)/2$	3. 6249	3. 9034
8	$E_{FL}=(E_{HOMO}+ E_{LUMO})/2$	-3. 6249	-3. 9034

 https://doi.org/10.37896/pd92.6/92618

ISSN: 0369-8963

UV-vis spectroscopic analysis

UV-vis calculations involve the excitation of an electron from the occupied orbital to a higher energy orbital. This excitation occurs when a photon with the energy that matches the difference between the two states interacts with the molecule. In our study, UV-vis spectra of isolated thiophene and analyte-bound complexes were simulated at the TD-DFT B3LYP/6-31+G(d) level. It is known that TD-DFT B3LYP energy values are very accurate and are always closer to the experimental values [46]. TD-DFT obtains the wave functions of MOs that oscillate between the ground and the first excited state. Figures 4(a) and 4(b) show the UV-vis spectra of isolated thiophene and the analyte-bound complex that represents the main peak positions and information regarding the observed shifts. In Table 8, we list the calculated maximum absorption wavelength λ_{max} [nm], vertical excitation energies (ΔE) [in eV], oscillator strengths, coefficients, and molecular orbitals of the allowed transitions involved in the excitation of thiophene and thiophene with COS.

In UV-vis spectroscopic analysis, the absorption spectrum of molecules is characterized by the vertical excitation energies. Table 8 lists the λ_{max} value of isolated thiophene that exhibits maximum absorbance at 215. 66nm. After complexation of thiophene with COS, the value of λ_{max} for the allowed transition of thiophene with COS is 262. 09nm. Further, from the results of TD-DFT, the vertical excitation energy of thiophene which corresponds to λ_{max} is 5. 75eV (ΔE). For thiophene with COS, the vertical excitation energy that corresponds to λ_{max} is 4. 73eV (ΔE). From our results, thiophene is red shifted upon interaction with COS (refer to Figures 4(a) and 4(b) and Table 8). The red shift is due to the doping process of thiophene by COS. COS donates an electron cloud to thiophene and decreases its energy gap. From Figures 4(a) and 4(b), it is observed that two distinct peaks are observed for isolated thiophene and two prominent peaks are observed for the monomer with the analyte. The monomer yields peaks at 215. 66nm and 186. 85nm, and the monomer with the analyte yields peaks at 262. 09nm and

 https://doi.org/10.37896/pd92.6/92618

ISSN: 0369-8963

223. 36nm. The major band peak of thiophene is red shifted from 215. 66nm to 262. 09nm upon interaction with COS. Thus, upon complexation of the monomer with the analyte, the λ_{max} value is red shifted, and all the electronic transitions involved are the π–π^* transitions.

The λ_{max} [nm] value of thiophene is equal to 215. 66nm, and the value corresponding to the vertical excitation energy of 5. 75eV is 0. 18eV smaller than the calculated λ_{max} [nm] value of the isolated thiophene (which has a value equal to 209. 22nm) and corresponds to a vertical excitation energy equal to 5. 93eV according to theTD-DFT B3LYP/6-31G(d), as suggested by Sajid et al. [13]. The small difference of 0. 18eV shows that our findings agree with the result obtained by Sajid et al. [13] at the TD-DFT B3LYP/6-31+G(d) level. Thus, our results indicate that the monomer with COS is responsible for shifting λ_{max} to longer wavelengths (red shift).

 https://doi.org/10.37896/pd92.6/92618

ISSN: 0369-8963

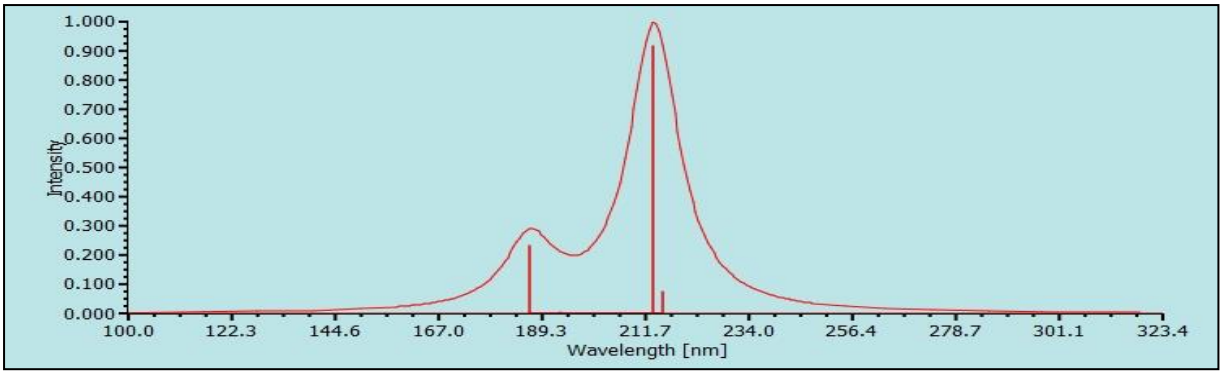

(a)

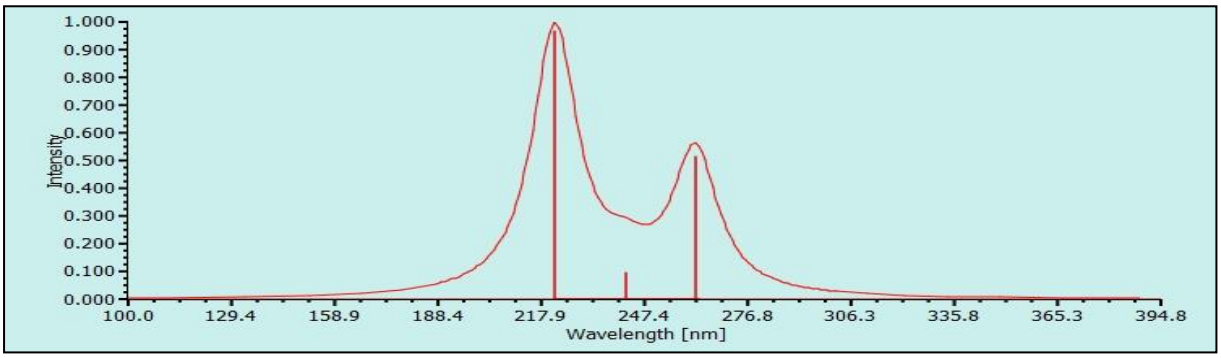

(b)

Figure 4. (a) Ultraviolet-visible (UV-vis) spectroscopic analysis of thiophene at the time-dependent (TD)-DFT B3LYP/6-31+G(d) level. (b)UV-vis spectroscopic analysis of thiophene with COS at the TD-DFT B3LYP/6-31+G(d) level

 https://doi.org/10.37896/pd92.6/92618

ISSN: 0369-8963

Table 8. Ultraviolet-visible spectroscopic analysis of isolated thiophene and thiophene with COS at the time-dependent (TD)-DFT B3LYP/6-31+G(d) level

Calculated maximum absorption wavelength, excitation energies, oscillator strengths, and molecular orbitals of the first allowed singlet transitions involved in the excitation of thiophene and thiophene with COS at the TD-DFT B3LYP/6-31+G(d) level

S. no	Parameter	Thiophene	Thiophene with COS	Result
1	Maximum absorption wavelength λ_{max} [nm]	215. 66	262. 09	Redshifted
2	Excitation energy(ΔE) [eV]	5. 75	4. 73	
3	Oscillator strength	0. 0073	0. 0016	
4	Coefficient	0. 6975	0. 7068	
5	Molecular orbitals (MOs)	22 $\longrightarrow$ 24	37 $\longrightarrow$ 39	

 https://doi.org/10.37896/pd92.6/92618

ISSN: 0369-8963

Infrared spectral characteristics

Computed IR spectra of thiophene, thiophene-COS are given in figures 5(a), and 5(b) respectively. The important peaks of thiophene and thiophene with COS along with their appropriate assignments are compared to their available experimental values [39] and are given in tables 9 (a) and 9 (b) respectively. The simulated scaled IR spectrum of thiophene has two prominent peaks in the functional group region at 695.92 cm^{-1} C-H wag out- of-plane (experimental 712cm^{-1}) and 805.33 cm^{-1} C-S str (experimental 839cm^{-1}). For thiophene with COS, 3 peaks appear in the functional groups at 700.44 cm^{-1} C-H wag out-of-plane (experimental 712cm^{-1}) , 806.17 cm^{-1} C-S str (experimental 839cm^{-1}) and a peak is observed at 2024.15 cm^{-1} due to C=O str of COS (experimental 2040 cm^{-1}). The results predict the vibrational characteristics of the complex. Comparison of the scaled frequencies of the thiophene and thiophene-COS [refer figures 5 (a), and 5 (b) and tables 9 (a) and 9 (b)] provide conclusion that COS adsorption causes a red shift in the frequencies of the finger print region of the complex than that of the monomer.

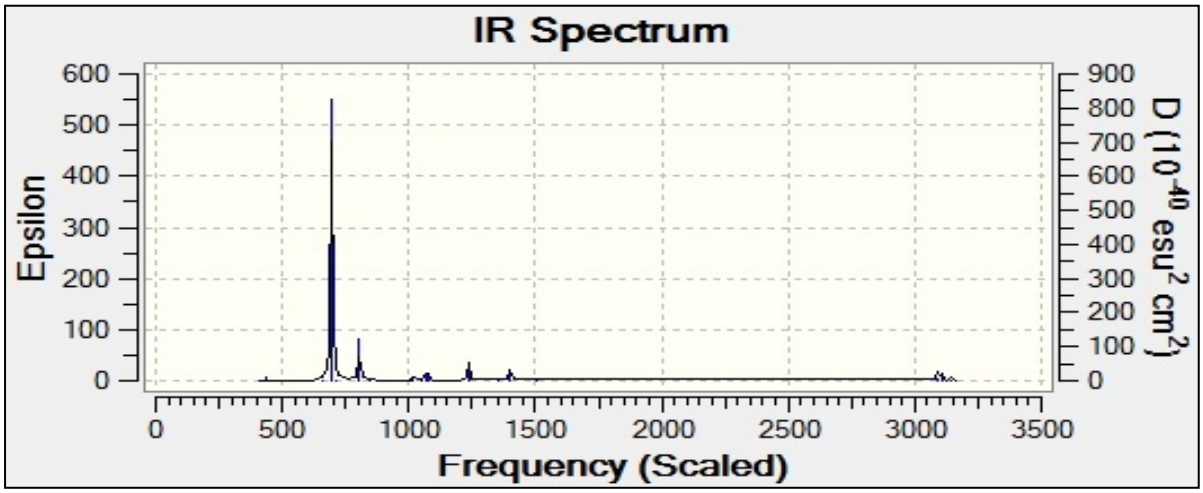

Figure 5(a) Scaled IR spectra of thiophene

https://doi.org/10.37896/pd92.6/92618

ISSN: 0369-8963

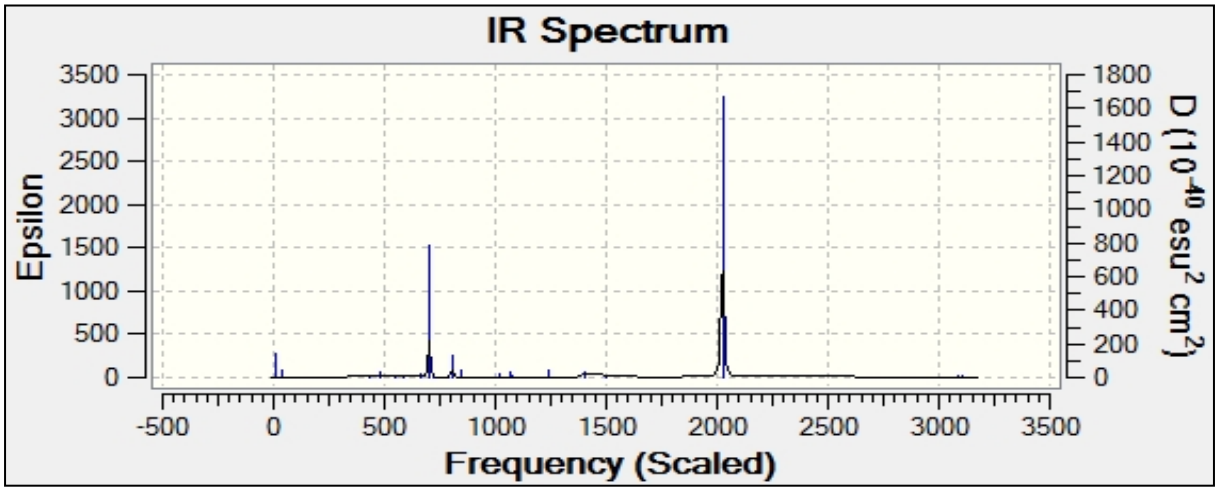

Figure 5 (b) Scaled IR spectra of thiophene with COS

Table 9 (a):-Calculated frequencies (in cm^{-1}) of thiophene

Experimental frequencies (in cm^{-1})	Calculated frequencies (in cm^{-1})		Appropriate assignments
	unscaled	scaled	
712	723.94	695.92	C-H wag out of plane
839	837.75	805.33	C-S str
1083	1117.21	1073.97	CCH bend in plane
1256	1286.39	1236.66	CCH bend in plane
1409	1458.32	1401.88	C=C, C-C,ring str
3126	3216.03	3091.57	C-H str

https://doi.org/10.37896/pd92.6/92618

ISSN: 0369-8963

Table 9 (b):-Calculated frequencies (in cm^{-1}) of thiophene with COS

Experimental frequencies (in cm^{-1})	Calculated frequencies (in cm^{-1})		Appropriate assignments
	unscaled	scaled	
712	728.64	700.44	C-H wag out of plane
839	838.62	806.17	C-S str
839	881.68	847.55	C-S str
1036	1057.58	1016.65	CCH bend; C-C str
1256	1286.21	1236.43	CCH bend in plane
1409	1458.95	1402.49	C=C,C-C,ring str
2040	2105.64	2024.15	C=O str
3126	3265.94	3139.55	C-H str

Conclusions

DFT studies of thiophene and its interactions with COS were conducted to investigate the gas-sensing properties of thiophene. Our studies predicted that thiophene may serve as an efficient gas sensor, promising to replace the conventional solid-state sensor. Further chronic exposure of COS may cause numerous health problems and the current study focused on the the interaction of COS with thiophene, and provides an indispensable way to monitor the concentration of the analyte and to assure environmental safety. Both the intermolecular interaction energy and the counterpoise-corrected energies were calculated and analyzed. The intermolecular interaction was found to be a weak van der Waals interaction, and the value of the adsorption energy was in the physisorption range. The doping level of thiophene was altered by the interaction of COS owing to the transfer of electrons from the analyte to the

 https://doi.org/10.37896/pd92.6/92618

ISSN: 0369-8963

monomer. Optimized geometric parameters and the electronic structure calculations before and after interaction were evaluated to analyze the sensitivity of thiophene with COS. The values of recovery time suggest the reusable efficiency of the thiophene/carbonyl sulphide gas sensor. The Mulliken and the NBO calculations quantified the amount of intermolecular charge transfer from the analyte to the monomer. Frontier molecular orbitals and their energy gaps before and after interaction confirmed the gas-sensing properties. The conductivity of the thiophene increased upon interaction with the analyte owing to the decrease in the energy gap value. The TD-DFT calculation shows that red shifting was observed in the UV-vis spectra upon interaction with the analyte. The global reactive indices and IR vibrational assignments indicated that thiophene can be potentially used as a gas sensor toward the detection of the gas analyte COS. The obtained results of the electronic structure calculations and the value of excitation energy demonstrated that the thiophene has good sensing ability. Further, the COS adsorption on thiophene causes a significant transfer of charge that determines the adsorption energy; in turn, this produces a change in the resistance of the host layer. Thus, our study provides a better understanding of the gas sensing mechanism of thiophene with COS. Thiophene is a promising material that can be researched further to explore its structural and electronic properties for various applications in organic semiconducting devices, and as a functional organic material for electronic and optical devices.

Acknowledgements

The authors are thankful to KCG College of Technology, Karapakkam, and Madras Christian College, Tambaram, for providing the computational facilities necessary for the pursuit and completion of this work.

 https://doi.org/10.37896/pd92.6/92618

ISSN: 0369-8963

Funding: No funding was obtained from funding agencies in the public, commercial, or not-for-profit sectors.

Declaration of interests: None.

References

[1] P. Haripriya, R. Amrutha, P. Chandran, Interaction Energy, Counterpoise-Corrected Energy, and Charge Transfer Thiophene Characteristics as Basis for its Potential Use as a Gas Sensor: A Density Functional Theory Approach. Available at SSRN: https://ssrn.com/abstract=4313989 or http://dx.doi.org/10.2139/ssrn.4313989

[2] L. Pan, H. Qiu, C. Dou, Y. Li, L. Pu, J. Xu, Y. Shi, Conducting polymer nanostructures: Template synthesis and applications in energy storage, Int. J. Mol. Sci. 11 (2010) 2636–2657.

[3] J. Janata, M. Josowicz, Conducting polymers in electronic chemical sensors, Nat. Mater. 2(2003)19–24.

[4] H. Yoon, Current trends in sensors based on conducting polymer nanomaterials, Nanomaterials (Basel) 3(2013)524–549.

[5] M. Gerard, A. Chaubey, B. D. Malhotra, Application of conducting polymers to biosensors, Biosens. Bioelectron. 17 (2002)345–359.

[6] A. Patra, M. Bendikov, Polyselenophenes, J. Mater. Chem. 20 (2010) 422–433.

[7] T. Patois, J. B. Sanchez, F. Berger, J. Y. Rauch, P. Fievet, B. Lakard, Ammonia gas sensors based on polypyrrole films: Influence of electrodeposition parameters, Sens. Actuators B 171-172 (2012)431-439.

[8] N. Kumar, S. R. Vadera, J. Singh, G. Das, S. C. Negi, P. Aparna, A. Tuli, Conducting Polymers. Emerging commercial materials, Def. Sci. J. 46 (1996) 91-104.

[9] H. Bai, G. Shi, Gas Sensors Based on Conducting Polymers, Sensors7(2007)267-307.

 https://doi.org/10.37896/pd92.6/92618

ISSN: 0369-8963

[10] S. Bibi, H. Ullah, S. M. Ahmad, A. U. H. Ali Shah, S. Bilal, A. A. Tahir, K. Ayub, Molecular and electronic structure elucidation of polypyrrole gas sensors, J. Phys. Chem. C119(2015).

[11] H. Ullah, A. U. H. A. Shah, S. Bilal, K. Ayub, DFT study of polyaniline NH_3, CO_2, and CO gas sensors: Comparison with recent experimental data, J. Phys. Chem. C. 117 (2013)23701-23711.

[12] A. S. Rad, P. Valipour, A. Gholizade, S. E. Mousavinezhad, Interaction of SO_2 and SO_3 on terthiophene (as a model of polythiophene gas sensor): DFT calculations, Chem. Phys. Lett. 639(2015)29-35.

[13] H. Sajid, T. Mahmood, K. Ayub, An accurate comparative theoretical study of the interaction of furan, pyrrole, and thiophene with various gaseous analytes, J. Mol. Model. 23(2017)1-18.

[14] A. Shokuhi Rad, Application of polythiophene to methanol vapor detection: an ab initio study, J. Mol. Model. 21(2015) 2–7.

[15] A. Shokuhi Rad, M. Esfahanian, E. Ganjian, H. Allah Tayebi, S. B. Novir, The polythiophene molecular segment as a sensor model for H_2O, HCN, NH_3, SO_3, and H_2S: a density functional theory study, J. Mol. Model. 22(2016) 1–8.

[16] P. Haripriya, R. Amrutha, P. Chandran, Density functional theory (DFT) and natural bond orbital (NBO) analysis of the interaction of carbonyl sulfide with thiophene as a gas sensor, Periodico di Mineralogia 91 (2022)886–918.

[17]C. P. Chengelis, R. A. Neal, Studies of carbonyl sulfide toxicity: Metabolism by carbonic anhydrase. Toxicol. Appl. Pharmacol. 55 (1980) 198–202.

[18]Office of Environmental Health Hazard Assessment, Air toxics hot spots program carbonyl sulfide reference exposure levels (2017).

 https://doi.org/10.37896/pd92.6/92618

ISSN: 0369-8963

[19] A. R. Bartholomaeus, V. S. Haritos, Review of the toxicology of carbonyl sulfide, a new grain fumigant. Food Chem. Toxicol. 43(2005)1687–1701.

[20] S. F. Watts, The mass budgets of carbonyl sulfide , dimethyl sulfide , carbon disulfide and hydrogen sulfide, Atmos.Environ. 34 (2000). 761–779.

[21] Hund, F. ZurDeutung der Molekelspektren. I. Z. Physik 40, (1927) 742–764.

[22] R. S. Mulliken, The assignment of quantum numbers for electrons in molecules. I Phys. Rev. 32(1928)186-222.

[23] J. E. Lennard-Jones, The electronic structure of some diatomic molecules, Trans. FaradaySoc. 25(1929)668–686.

[24]M. J. Frisch, G. W. Trucks, H. B. Schlegel, G. E. Scuseria, M. A. Robb, J. R. Cheeseman, G. Scalmani, V. Barone, B. Mennucci, G. A. Petersson, H. Nakatsuji, M. Caricato, X. Li, H. P. Hratchian, A. F. Izmaylov, J. Bloino, G. Zheng, J. L. Sonnenberg, M. Hada, M. Ehara, K. Toyota, R. Fukuda, J. Hasegawa, M. Ishida, T. Nakajima, Y. Honda, O. Kitao, H. Nakai, T. Vreven, J. A. Montgomery, Jr. , J. E. Peralta, F. Ogliaro, M. Bearpark, J. J. Heyd, E. Brothers, K. N. Kudin, V. N. Staroverov, R. Kobayashi, J. Normand, K. Raghavachari, A. Rendell, J. C. Burant, S. S. Iyengar, J. Tomasi, M. Cossi, N. Rega, J. M. Millam, M. Klene, J. E. Knox, J. B. Cross, V. Bakken, C. Adamo, J. Jaramillo, R. Gomperts, R. E. Stratmann, O. Yazyev, A. J. Austin, R. Cammi, C. Pomelli, J. W. Ochterski, R. L. Martin, K. Morokuma, V. G. Zakrzewski, G. A. Voth, P. Salvador, J. J. Dannen- berg, S. Dapprich, A. D. Daniels, Ö. Farkas, J. B. Foresman, J. V. Ortiz, J. Cio- slowski, and D. J. Fox, Gaussian, Inc. , Wallingford CT, 2009.

[25] R. Dennington, T. Keith, J. Millam J, GaussView 5. 0. Wallingford, CT, USA, SemichemInc, Shawnee Mission, KS, ISBN: 978-1-935522-00- Updated on: 9 Jun 2009 (2009).

 https://doi.org/10.37896/pd92.6/92618

ISSN: 0369-8963

[26] A. R. Allouche, Gabedit-A graphical user interface for computational chemistry softwares, J. Comput. Chem. 32(2011)174–182.

[27] N. Mardirossian, M. Head-Gordon, Thirty years of density functional theory in computational chemistry: An overview and extensive assessment of 200 density functionals, Mol. Phys. 115, (2017) 2315–2372.

[28] S. Grimme, Density functional theory with London dispersion corrections. Wiley Interdiscip. Rev. Comput. Mol. Sci. 1(2011)211–228.

[29] A. D. Boese, Density functional theory and hydrogen bonds: Are we there yet? Chem. Phys. Chem. 16(2015)978–985.

[30] A. D. Becke, Density-functional thermochemistry. III. The role of exact exchange, J. Chem. Phys. 98(1993) 5648–5652.

[31] A. D. Becke, Density-functional exchange-energy approximation with correct asymptotic behavior, Phys. Rev. A38(1998)3098–3100.

[32] C. Lee, W. Yang, R. G. Parr, Development of the Colle–Salvetti correlation-energy formula into a functional of the electron density, Phys. Rev. B 37(1988)785–789.

[33] B. Miehlich, A. Savin, H. Stoll, H. Preuss, Results obtained with the correlation energy density functionals of becke and Lee, Yang and Parr, Chem. Phys. Lett. 157(1989)200–206.

[34] R. Amrutha, P. Haripriya, S. Lakshmi, P. Chandran, A molecular orbital calculation on the structures of mono and dihydroxy benzenes and their halogen substituted species. Indian J. Chem. - Sect. A Inorganic, Phys. Theor. Anal. Chem. 46 (2007)729–735.

[35] J. H. Li, J. Wu, Y. X. Yu, DFT exploration of sensor performances of two-dimensional WO3 to ten small gases in terms of work function and band gap changes and I-V responses. Appl. Surf. Sci. 546(2021)1-11.

[36] A. Shokri, N. Salami, Gas sensor based on MoS_2 monolayer, Sensors Actuators, B Chem. 236, (2016) 378–385.

 https://doi.org/10.37896/pd92.6/92618

[37] F. C. Franco, Interaction of several toxic heterocarbonyl gases with polypyrrole as a potential gas sensor. Chemosensors 8(2020)84.

[38] D. R. L. Ed, CRC Handbook of Chemistry and Physics, 84th ed. , CRC Press LLC, Boca Raton, FL, US2004.

[39] M. Szajda, J. N. Lam, 2. 09 - Thiophenes and their Benzo Derivatives: Structure, ISBN 9780080965185, (1996), 437-490.

[40] X. Gao, Q. Zhou, J. Wang, L. Xu, W. Zeng, Performance of intrinsic and modified graphene for the adsorption of H_2S and CH_4: A DFT study, Nanomaterials (Basel) 10(2020)299.

[41]Computational chemistry comparison and benchmark, Database. https://cccbdb. nist. gov/nure1x. asp.

[42] T. Koopmans, Ordering of wave functions and eigen energies to the individual electrons of an atom, Physica1 (1933)104–113.

[43] A. Shokuhi, S. Sadeghi, S. Mohseni, S.Aghouzi,Study on the adsorption properties of O_3 , SO_2 , and SO_3 on B-doped graphene using DFT calculations. J. Solid State Chem. 237, (2016) 204–210.

[44] R. G. Parr, LvSzentpály, S. Liu, Electrophilicity index, J. Am. Chem. Soc. 121(1999)1922–1924.

[45] A. Mubarik, N. Rasool, M. A. , A. Hashmi, M. Mansha, M. R. Zubair, M. A. F. Shaik, E. M. Sharaf, A. Awwad, Abdelgawad, Computational study of structural, molecular orbitals, optical and thermodynamic parameters of thiophene sulfonamide derivatives, Crystals, 11(2021*)* 211.

[46] G. A. Hudson, L. Cheng, J. Yu, Y. Yan, D. J. Dyer, M. E. , L. Mc Carroll, Wang, Computational studies onresponse and binding selectivity of fluorescence sensors, J. Phys. Chem. B. 114 (2010)870–876.

 https://doi.org/10.37896/pd92.6/92618